applied sciences

MDPI

Article

Tunable Plasmonic Resonance Sensor Using a Metamaterial Film in a D-Shaped Photonic Crystal Fiber for Refractive Index Measurements

Markos Paulo Cardoso [1,*], Anderson O. Silva [2], Amanda F. Romeiro [1], Maria Thereza R. Giraldi [3], João C. W. Albuquerque Costa [1], José L. Santos [4,5], José M. Baptista [4,6] and Ariel Guerreiro [4,5]

[1] Applied Electromagnetism Laboratory, Federal University of Pará, Belém 66075-110, Brazil; romeiro.amanda@gmail.com (A.F.R.); jweyl@ufpa.br (J.C.W.A.C.)
[2] Federal Center for Technological Education Celso Suckow da Fonseca, Rio de Janeiro 22743-041, Brazil; anderson.silva@cefet-rj.br
[3] Laboratory of Photonics, Military Institute of Engineering, Rio de Janeiro 22290-270, Brazil; mtmrocco@gmail.com
[4] INESC TEC, 4200-465 Porto, Portugal; josantos@fc.up.pt (J.L.S.); jmb@inesctec.pt (J.M.B.); ariel@fc.up.pt (A.G.)
[5] Faculty of Sciences, University of Porto, 4099-002 Porto, Portugal
[6] Faculty of Exact Sciences and Engineering, University of Madeira, 9020-105 Funchal, Portugal
* Correspondence: markos.cardoso@itec.ufpa.br

Abstract: Subwavelength cells of metallic nanorods arrayed in a dielectric background, termed "metamaterials", present bulk properties that are useful to control and manipulate surface plasmon resonances. Such feature finds tremendous potential in providing a broad manifold of applications for plasmonic optical sensors. In this paper, we propose a surface-plasmon-resonance-based sensor with spectral response tunable by the volume fraction of silver present in a metamaterial layer deposited on a D-shaped photonic crystal fiber. Using computational simulations, we show that sensitivity and resolution can be hugely altered by changing the amount of constituents in the metamaterial, with no further modifications in the structure of the sensor. Moreover, the designed sensor can also be applied to label the average volume fraction of silver in the metamaterial layer and then to estimate its effective constitutive parameters.

Keywords: surface plasmon resonance; photonic crystal D-shaped fiber; refractive index sensor; metamaterial; tunable sensor

check for updates

Citation: Cardoso, M.P.; Silva, A.O.; Romeiro, A.F.; Giraldi, M.T.R.; Costa, J.C.W.A.; Santos, J.L.; Baptista, J.M.; Guerreiro, A. Tunable Plasmonic Resonance Sensor Using a Metamaterial Film in a D-Shaped Photonic Crystal Fiber for Refractive Index Measurements. *Appl. Sci.* **2022**, *12*, 2153. https://doi.org/10.3390/app12042153

Academic Editors: Francisco Pérez-Ocón and Alessandro Belardini

Received: 12 January 2022
Accepted: 15 February 2022
Published: 18 February 2022

1. Introduction

Electromagnetic modes arising from the coupling between photons and free-electron oscillations at a conducting surface, also known as surface plasmons-polaritons, introduced a revolution in the field of optical sensing. The engineering of surface plasmon resonance (SPR)-based devices has increased dramatically the levels of resolution and sensitivity typically provided by conventional optical sensors [1]. A wide variety of configurations have been proposed to reach the SPR condition: optical fibers with cladding partially removed for the deposition of a conducting layer as tapered fibers, grating-based fibers, and D-shaped fibers [2–4]. Notably, photonic crystal fibers (PCFs) are frequently employed to excite SPR modes due to their unique features, such as fine control of the evanescent field penetration in the conducting medium and high mode confinement within a large mode area [5–7].

The characteristics of an SPR sensor rely on the dependence of the optical fields associated with the plasmon mode on the geometry and nature of the conducting layer as well as on the refractive index of the surrounding media (also known as analyte). Small variations in the refractive index of the analyte change significantly the mode phase and losses of the surface plasmon mode. This dependence can be tailored with the application of optical metamaterials, artificial structured media designed to achieve a set of properties not typically found in nature. The lattice of such materials has dimensions many orders of magnitude smaller than the optical wavelength, and thus the light propagation through the entire medium can be described by effective constitutive parameters. For instance, field enhancement can be favored in a large extent when metamaterials with metallic inclusions are used in the construction of a compacted optical sensor [8–10], thus providing an alternative to plasmonic sensors composed of metallic films [4–11] or individual metallic nanostructures on optical fibers, the latter typically harder to simulate and fabricate [12].

This paper reports the design of an SPR sensor based on a D-shaped PCF with a metamaterial film for detection of the refractive index. The metamaterial layer is composed of an array of silver nanorods embedded in an alumina matrix. This type of metamaterial, generally called wire metamaterial, resembles a crystalline lattice with the optical axis along the axial direction of the nanorods [10]. The bulk optical modes result from the coupling between surface plasmons locally excited at a unitary cell when the electric field is polarized along the optical axis. The sensitivity is taken from the spectral shifts of the resonance absorption peaks upon changes in the refractive index of the analyte. We address the dependence of the resonance wavelengths on the amount of silver nanorods embedded in alumina, showing that the SPR spectral channels can be tuned by the filling ratio of the metamaterial. As a consequence, we demonstrate that a linear relationship between the SPR spectral response and the volume ratio of silver in the metamaterial can be accurately regarded to characterize effective optical properties of the metamaterial. In the following sections, we detail the modeling of the SPR sensor based on a D-shaped PCF and discuss the application of the tunable spectral sensing response.

2. Design and Model

The proposed sensor is schematically depicted in Figure 1. The total diameter of the fiber was D = 24 μm. The PCF cross section was composed of a hexagonal array of air holes in a silica background (Figure 1a). The diameter of the fiber core was 5 μm, and the distance between two adjacent air holes was Λ = 2 μm. The diameter d of each air hole was obtained from the ratio d/Λ = 0.88. The D-shaped structure can be fabricated by the stack-and-draw technique [13]. A metamaterial layer composed of silver nanorods embedded in an alumina matrix was deposited on the flat surface of the fiber. Its total width and thickness were 10 μm and 40 nm, respectively. Figure 1b highlights the metamaterial structure.

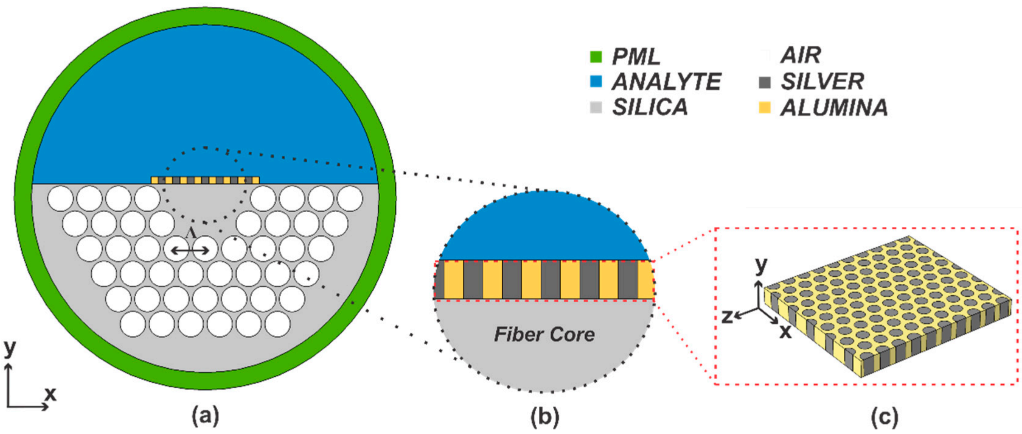

Figure 1. D-shaped photonic crystal fiber with a metamaterial layer. (**a**) Cross section of the sensor with total diameter D = 24 μm and Λ = 2 μm. The diameter d of each air hole was obtained from the ratio d/Λ = 0.88. The outermost layer that encloses the entire domain corresponds to a 0.1 D-thick PML. (**b**) A closer view of the orientation of the silver nanowires in the metamaterial layer with respect to the flat face of the D-shaped PCF. (**c**) A perspective view of the metamaterial layer deposited on the top of the flat face of the PCF. The layer is 10 μm width and 40 nm thick.

For accurate modeling at the optical spectral range, the dispersive characteristics of all materials in the sensing structure had to be considered. The refractive index of silica was computed from the Sellmeier equation [14], and the air region was modeled by a constant refractive index n_{air} = 1. The metamaterial was described in terms of its effective bulk permittivity, which was computed from Maxwell–Garnett theory (MGT) [15]:

$$\varepsilon = \varepsilon_h \frac{1 + 2f\frac{\varepsilon_1 - \varepsilon_h}{\varepsilon_1 + 2\varepsilon_h}}{1 - f\frac{\varepsilon_1 - \varepsilon_h}{\varepsilon_1 + 2\varepsilon_h}}. \tag{1}$$

where ε_1 corresponds to the permittivity of silver nanorod inclusions and ε_h is the permittivity of the alumina host medium.

In general, MGT does not properly retrieve the effective constitutive parameters of media with an arrayed set of large inclusions due to disregarding multipole interactions between local fields [15–17]. In uniaxial media, however, this analytical model remains valid to describe lightwave couplings that are direct contributions from local modes excited along the optical axis [18–20]. Since the surface plasmon modes at the flat interface between the D-shaped PCF and a conductive layer are excited by the fiber mode polarized perpendicularly to the interface [4,11], the plasmonic resonances derive from the local plasmon modes excited along the optical axis of the nanowire medium in the case of the geometric configuration displayed in Figure 1, preserving the accuracy of the Maxwell–Garnett formalism for the homogenization of the metamaterial.

In Equation (1), the filling factor f represents the fractional volume of silver that composes the metamaterial lattice. The dispersive permittivity of silver was obtained from the corrected version of the Drude–Lorentz model [11]:

$$\varepsilon_{Ag}(\omega) = \varepsilon_\infty - \frac{\omega_p^2}{\omega(\omega + i\gamma)} - \frac{\Delta\epsilon\Omega_L^2}{\left(\omega^2 - \Omega_L^2\right) + i\omega\Gamma_L} \tag{2}$$

The parameters ω_p = 2155.6 THz and γ = 15.92 THz are the plasma frequency and damping factor, respectively, and ε_∞ = 5.9673 stands for the residual polarization of silver at high frequencies. The parameters in the correction factor are $\Delta\epsilon$ = 1.09, Ω_L = 650.07 THz, and Γ_L = 104.86 THz [21].

To evaluate the spectral output of the SPR sensor, we carried out numerical modeling of the effective guided modes using the finite element method software COMSOL Multiphysics [22]. The two-dimensional computational domain is given by the cross section of Figure 1a, truncated by a perfectly matched layer (PML) with a thickness of 0.1D (D is the diameter of the D-shaped PCF). The Wave Optics package in the frequency domain was applied to calculate the eigenvalues of the Helmholtz equation in the angular frequency ω:

$$\nabla_\perp^2 E(r_\perp, \omega) + k_0^2\left(\varepsilon(\omega) - n_{eff}^2\right)E(r_\perp, \omega) = 0, \tag{3}$$

where k_0 is the magnitude of the free-space wavenumber and ε is the complex frequency-dependent relative permittivity. $E(r_\perp, \omega)$ is the modal electric field distribution at the position $r_\perp$ perpendicular to the direction of light propagation. The expression for ε depends on the region at which Equation (2) is solved. In turn, the complex effective index n_{eff} is related to the mode resulting from the coupling between the fundamental fiber mode and the surface plasmon mode at the boundaries of the metamaterial layer. The real part of n_{eff} refers to the mode phase, and the imaginary part is related to the losses experienced by the confined mode as the fields are tunneled through the metamaterial interfaces.

3. Results

The SPR condition occurs when the phase of the fundamental fiber mode matched the phase of the surface plasmon at the metamaterial interface. At this coupling, the modal confinement losses reached a peak, as exemplified in Figure 2 for a metamaterial layer with filling fraction $f = 0.5$ and refractive index of the analyte $Ri_{analyte} = 1.33$. The confinement losses of the sensor could be calculated by [23]:

$$\alpha = 8686 \times 2\pi/\lambda \times Im_{neff} \times 10^4 \left(\frac{\text{dB}}{\text{cm}}\right), \tag{4}$$

where λ represents the wavelength and Im_{neff} is the imaginary part of the effective modal index.

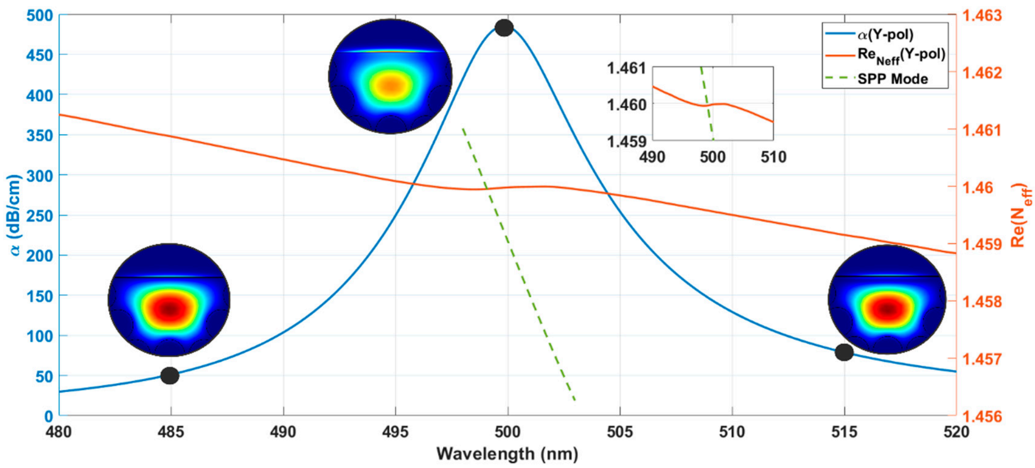

Figure 2. Dispersion curve of the fundamental fiber mode and SPP modes for a refractive index $Ri_{analyte} = 1.33$. Y-$_{\text{pol}}$ is the perpendicular polarization to the metamaterial film. The insets show the intersections between the dispersion curve of the fundamental Y-$_{\text{pol}}$ fiber mode and the plasmonic mode at the metamaterial interface.

The effective constitutive optical relations that characterize the wire metamaterial resulted from the coupling between surface plasmons excited by the electric field with polarization parallel to the optical axis. Therefore, only the electric field oriented perpendicularly to the metamaterial interface (y axis direction in Figure 1a) allows for the excitation of plasmonic modes, even though the fundamental mode of the PCF is degenerate for two orthogonal polarizations.

The variation of the refractive index of the analyte changed the SPR wavelength as well as the magnitude of the confinement losses. Figure 3 shows the confinement loss spectra presented by the D-shaped PCF with a metamaterial layer regarding a filling fraction $f = 0.3$ and refractive indexes of the analyte in the range of 1.30–1.39.

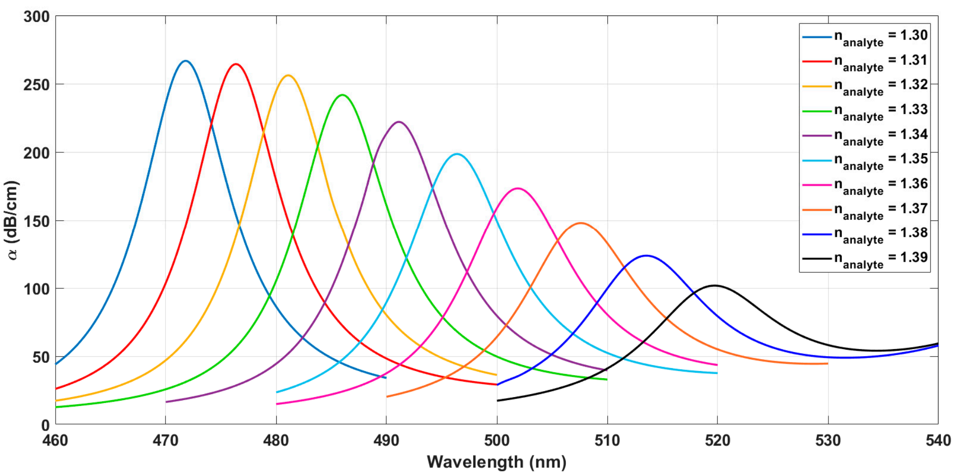

Figure 3. Confinement loss spectra for different analyte refractive indexes for the D-shaped fiber with a metamaterial with filling factor $f = 0.3$.

The tunable spectral sensing response of the D-shaped PCF with the metamaterial was accounted by the sensitivity S estimated as the average change in the SPR wavelength with the change in the refractive index of the analyte [24]:

$$S = \Delta\lambda_{peak}/\Delta n_{analyte}\ (\mathrm{nm/RIU}) \quad (5)$$

where $\Delta\lambda_{peak}$ is the wavelength resonance displacement and $\Delta n_{analyte}$ is defined as the changes in the analyte refractive index. Correspondingly, regarding an optical spectrum analyzer of minimal detectable change $\Delta\lambda_{min} = 0.1$nm in the SPR loss spectra [25–27], the resolution associated to S could be expressed by:

$$R = \Delta n_{analyte} \times \left(\Delta\lambda_{min}/\Delta\lambda_{peak}\right)\ (\mathrm{RIU}) \quad (6)$$

From the spectra shown in Figure 3, the obtained sensitivity and resolution were 532 nm/RIU and 1.8789×10^{-4} RIU, respectively.

The fractional volume of constituents modified the conductive character of the metamaterial. Figure 4 displays the distribution of electric field intensity at the SPR wavelength for three different volume fractions of silver in the metamaterial layer. In all cases, surface plasmon resonance was achieved at the optimal coupling between the Y-polarized fundamental fiber mode and the surface mode at the metamaterial interface; however, the field enhancement at the resonance wavelength benefited from a major amount of metallic inclusions. The net consequence was a shifting of the SPR spectra according to different filling fractions of silver in the metamaterial layer. Therefore, the spectral range for the sensor operation and even the sensitivity levels can be tuned by modifying the volume fraction of silver embedded in alumina.

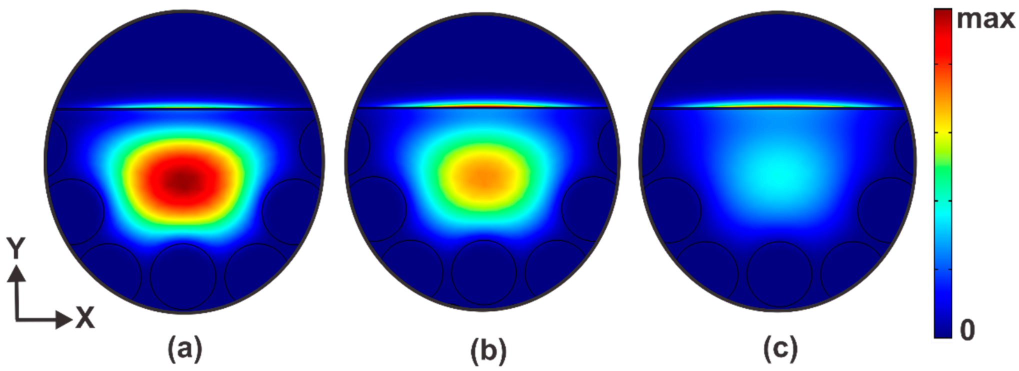

Figure 4. Distribution of the Y-polarized electric field intensity at the SPR wavelength λ_p for three different silver volume fractions: (**a**) $f = 0.3$ at λ_p = 485 nm, (**b**) $f = 0.5$ at λ_p = 500 nm, and (**c**) $f = 0.7$ at λ_p = 514 nm.

Figure 5 depicts the influence of the metamaterial filling fraction on the amplitude and spectral location of the confinement loss peak regarding a constant refractive index of the analyte, $Ri_{analyte} = 1.33$.

The tunable sensing response of the D-shaped PCF with the metamaterial is illustrated in Figure 6, in which the sensitivity and resolution were estimated from the linear fitted curve. In both cases, the determination coefficient was greater than 0.98, indicating that the modeled sensing structure can be accurately regarded as linear. For refractive indexes ranging from 1.30 to 1.39, the average sensitivity increased more than five times and resolution reached 10^{-5} RIU in order of the magnitude as the fractional volume of silver in the metamaterial changed from 0.3 to 0.7.

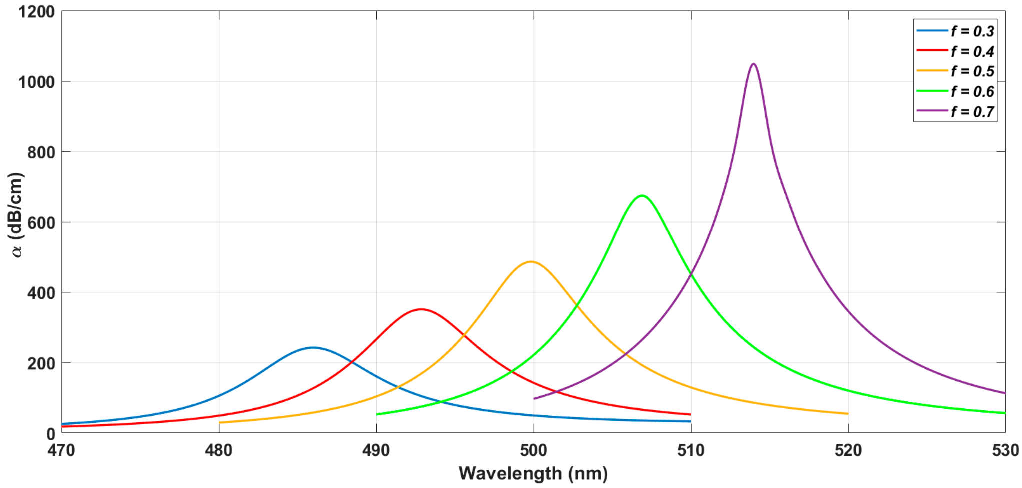

Figure 5. Confinement loss spectra for different filing factors and a constant refractive index of the analyte, $Ri_{analyte} = 1.33$.

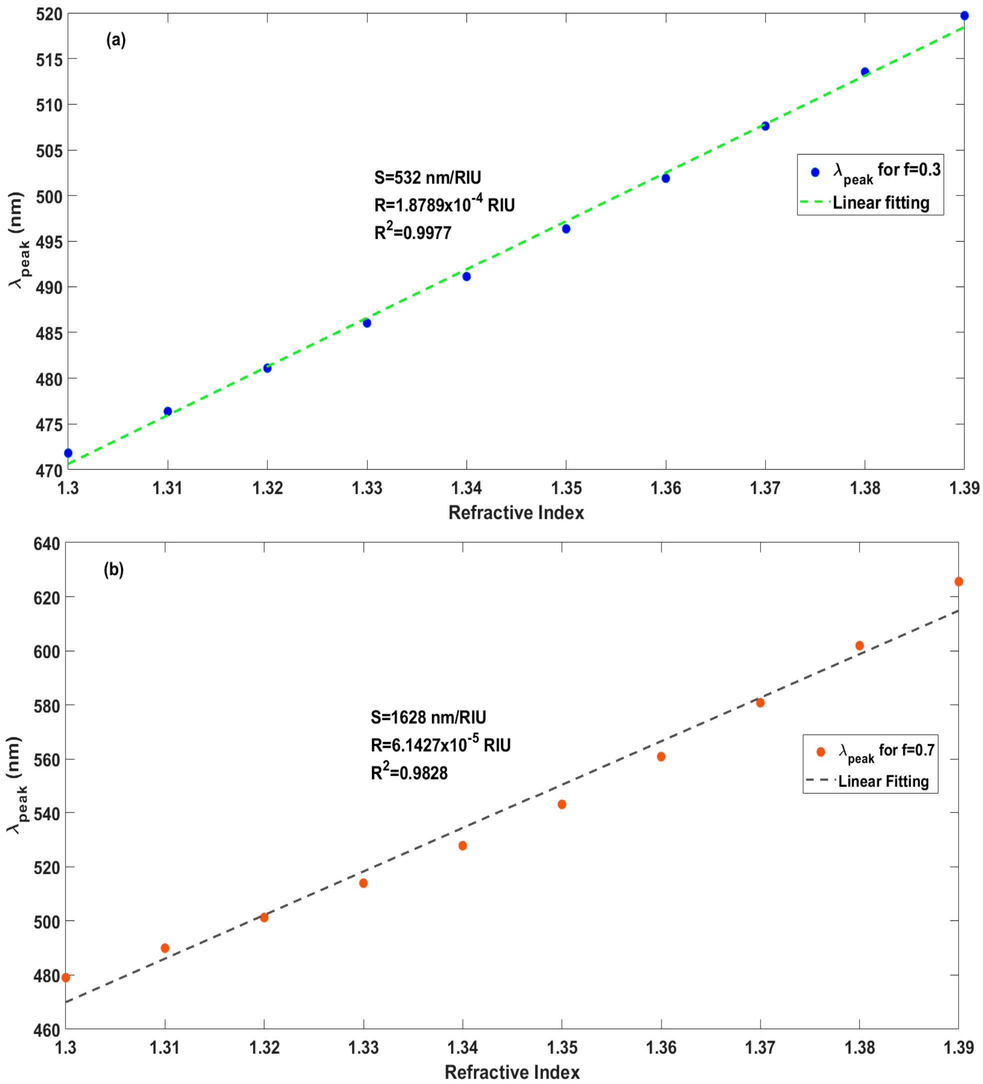

Figure 6. Variations of the SPR wavelength with the refractive index of the analyte obtained for volume fractions of silver in the metamaterial: (**a**) f = 0.3 and (**b**) f = 0.7.

In contrast, the shift of the SPR spectrum with the variations in the filling ratio of silver in the metamaterial enabled the designed sensor to estimate metamaterial constitutive parameters, which is particularly attractive to characterize effective properties of metamaterial samples whose constituents are not uniformly distributed [10].

Figure 7 shows that the spectral shifts of the SPR wavelength and the corresponding variation of the sensitivity with the fractional volume of silver in the metamaterial layer were approximately linear. In other words, the refractive index SPR sensor can depict the amount of metamaterial constituents from a proportional relation between sensitivity and ratio of metallic inclusions, which is of major importance to estimate bulk optical properties of the nanowire metamaterial.

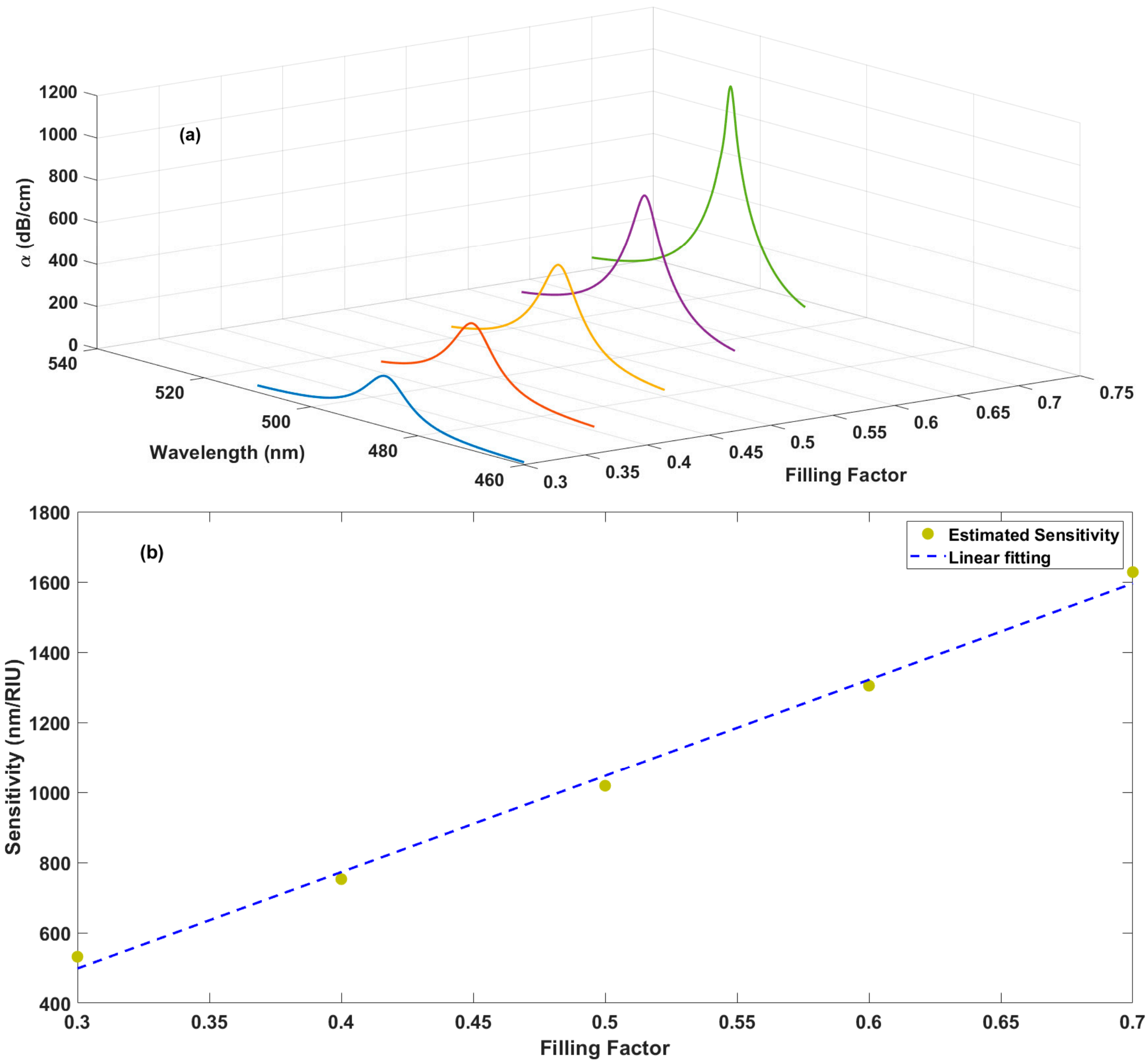

Figure 7. (**a**) SPR spectra tuned according to the filling factor of silver in the metamaterial layer obtained for an analyte with refractive index $Ri_{analyte} = 1.33$. (**b**) Sensitivity estimated for different filling factors.

4. Conclusions

This paper presented an approach to tune the spectra of a refractive index SPR sensor according to the ratio of inclusions in a nanowire metamaterial. The sensing platform was based on a D-shaped PCF covered by a metamaterial layer of silver nanorods embedded in an alumina matrix. The computed results showed a relationship approximately linear between the SPR spectra and refractive indexes in the range of 1.30–1.39. The plasmonic resonances were tunable according to the amount of silver in the metamaterial, resulting in a sensitivity linearly dependent on the fractional volume of metallic inclusions. Such linear relationship characterizes the designed SPR sensor as a suitable tool to unambiguously estimate the effective constitutive parameters of the metamaterial. Within a general framework, the proposed fiber-based sensing platform is an optimized scheme to biunivocally associate the SPR sensitivity to the volume ratio of metamaterial constituents without requiring any change in the structural parameters of the D-shaped PCF.

Author Contributions: Writing—review & editing, M.P.C., A.O.S., A.F.R., M.T.R.G., J.C.W.A.C., J.L.S., J.M.B. and A.G. All authors have read and agreed to the published version of the manuscript.

Funding: This study was financed, in part, by the Coordenação de Aperfeiçoamento de Pessoal de Nível Superior—Brazil (CAPES; finance code 001). During the period of elaboration of this work, the authors also obtained support from the Conselho Nacional de Desenvolvimento Cientifico e Tecnologico (CNPq), Brazil. It was also financed by the European Regional Development Fund (ERDF) through the Operational Program for Competitiveness and Internationalization—COMPETE 2020 Program and by national funds through the Portuguese funding agency Fundação para a Ciência e a Tecnologia (FCT) within the project "GreenNanoSensing" (POCI-01-0145-FEDER-032257).

Institutional Review Board Statement: Not applicable.

Informed Consent Statement: Not applicable.

Data Availability Statement: The data that support the findings of this study are available from the corresponding author upon reasonable request.

Conflicts of Interest: The authors declare no conflict of interest.

References

1. Homola, J. Surface Plasmons on Waveguides with a Perturbed Refractive Index Profile. In *Surface Plasmon Polariton Based Sensors*, 1st ed.; Springer: Berlin/Heidelberg, Germany; New York, NY, USA, 2018; Volume 4, pp. 19–26.
2. Lin, H.-Y.; Huang, C.-H.; Cheng, G.-L.; Chen, N.-K.; Chui, H.-C. Tapered optical fiber sensor based on localized surface plasmon resonance. *Opt. Express* **2012**, *20*, 21693–21701. [CrossRef]
3. Homola, J.; Koudela, I.; Yee, S.S. Surface plasmon resonance sensors based on diffraction gratings and prims couplers: Sensitivity comparison. *Sens. Actuators B Chem.* **1999**, *54*, 16–24. [CrossRef]
4. Cardoso, M.; Silva, A.; Romeiro, A.; Giraldi, M.; Costa, J.; Santos, J.; Baptista, J.; Guerreiro, A. Second-Order Dispersion Sensor Based on Multi-Plasmonic Surface Resonances in D-Shaped Photonic Crystal Fibers. *Photonics* **2021**, *8*, 181. [CrossRef]
5. Yu, X.; Zhang, Y.; Pan, S.; Shum, P.; Yan, M.; Leviatan, Y.; Li, C. A selectively coated photonic crystal fiber based surface plasmon resonance sensor. *J. Opt.* **2010**, *12*, 015005. [CrossRef]
6. Rifat, A.A.; Ahmed, R.; Yetisen, A.K.; Butt, H.; Sabouri, A.; Mahdiraji, G.A.; Yun, S.H.; Adikan, F.M. Photonic crystal fiber based plasmonic sensors. *Sens. Actuators B Chem.* **2017**, *243*, 311–325. [CrossRef]
7. Rifat, A.A.; Haider, F.; Ahmed, R.; Mahdiraji, G.A.; Adikan, F.R.M.; Miroshnichenko, A. Highly sensitive selectively coated photonic crystal fiber-based plasmonic sensor. *Opt. Lett.* **2018**, *43*, 891–894. [CrossRef]
8. Santos, D.; Guerreiro, A.; Baptista, J. SPR optimization using metamaterials in a D-type PCF refractive index sensor. *Opt. Fiber Technol.* **2017**, *33*, 83–88. [CrossRef]
9. Leite, I.T.; Hierro-Rodríguez, A.; Silva, A.O.; Teixeira, J.M.; Sousa, C.T.; Fernández-García, M.P.; Araújo, J.P.; Jorge, P.A.S.; Guerreiro, A. Exciting the optical response of nanowire metamaterial films on the tip of optical fibres. *Phys. Status Solidi Rapid Res. Lett.* **2013**, *7*, 664–667. [CrossRef]
10. Hierro-Rodriguez, A.; Rocha-Rodrigues, P.; Valdés-Bango, F.; Alameda, J.M.; Jorge, P.A.S.; Santos, J.L.; Araujo, J.P.; Teixeira, J.M.; Guerreiro, A. On the anodic aluminium oxide refractive index of nanoporous templates. *J. Phys. D Appl. Phys.* **2015**, *48*, 455105. [CrossRef]
11. Cardoso, M.P.; Silva, A.O.; Romeiro, A.F.; Giraldi, M.T.R.; Costa, J.C.; Santos, J.L.; Baptista, J.M.; Guerreiro, A. Multi-Plasmonic Resonance Based Sensor for the Characterization of Optical Dispersion Using a D-Shaped Photonic Crystal Fiber. *IEEE Instrum. Meas. Mag.* **2021**, *24*, 63–68. [CrossRef]
12. Guerreiro, A.; Santos, D.; Baptista, J.M. New Trends in the Simulation of Nanosplasmonic Optical D-Type Fiber Sensors. *Sensors* **2019**, *19*, 1772. [CrossRef] [PubMed]
13. Mahdiraji, G.A.; Chow, D.; Sandoghchi, S.R.; Amirkhan, F.; Dermosesian, E.; Yeo, K.S.; Kakaei, Z.; Ghomeishi, M.; Poh, S.Y.; Gang, S.Y.; et al. Challenges and Solutions in Fabrication of Silica-Based Photonic Crystal Fibers: An Experimental Study. *Fiber Integr. Opt.* **2014**, *33*, 85–104. [CrossRef]
14. Sharma, A.K.; Gupta, B.D. On the performance of different bimetallic combinations in surface plasmon resonance based fiber optic sensors. *J. Appl. Phys.* **2007**, *101*, 093111. [CrossRef]
15. Wenshan, C.; Shalaev, V. *Optical Metamaterials—Fundamentals and Applications*, 1st ed.; Springer: New York, NY, USA, 2010.

16. Belyaev, B.A.; Tyurnev, V.V. Electrodynamic Calculation of Effective Electromagnetic Parameters of a Dielectric Medium with Metallic Nanoparticles of a Given Size. *J. Exp. Theor. Phys.* **2018**, *127*, 608–619. [CrossRef]
17. Costa, J.S.; Zaman, Q.; Da Costa, K.Q.; Dmitriev, V.; Pandoli, O.; Fontes, G.; Del Rosso, T. Limits of the Effective Medium Theory in Particle Amplified Surface Plasmon Resonance Spectroscopy Biosensors. *Sensors* **2019**, *19*, 584. [CrossRef]
18. Leite, I.T.; Silva, A.O.; Hierro-Rodríguez, A.; Sousa, C.T.; Fernández-García, M.P.; Teixeira, J.M.; Araujo, J.P.; Giraldi, M.T.; Costa, J.W.C.A.; Viegas, D.; et al. Ag-nanowire metamaterials: Spectral reflectance analysis and homogenization models. In Proceedings of the 8th Ibero American Optics Meeting and 11th Latin American Meeting on Optics, Lasers, and Applications, Porto, Portugal, 22–26 July 2013.
19. Hierro-Rodriguez, A.; Leite, I.T.; Rocha-Rodrigues, P.; Fernandes, P.; Araujo, J.P.; Jorge, P.A.S.; Santos, J.L.; Teixeira, J.M.; Guerreiro, A. Hydrogen sensing via anomalous optical absorption of palladium-based metamaterials. *Nanotechnology* **2016**, *27*, 185501. [CrossRef]
20. Joannopoulos, J.D.; Johnson, S.G.; Winn, J.N.; Meade, R.D. *Photonic Crystal: Molding the Flow of Light*, 2nd ed.; Princeton University Press: Princeton, NJ, USA, 2008.
21. Vial, A.; Grimault, A.-S.; Macías, D.; Barchiesi, D.; de la Chapelle, M.L. Improved analytical fit of gold dispersion: Application to the modeling of extinction spectra with a finite-difference time-domain method. *Phys. Rev. B* **2005**, *71*, 085416. [CrossRef]
22. Comsol. Available online: www.br.comsol.com (accessed on 12 October 2021).
23. Luan, N.; Wang, R.; Lv, W.; Yao, J. Surface plasmon resonance sensor based on D-shaped microstructured optical fiber with hollow core. *Opt. Express* **2015**, *23*, 8576–8582. [CrossRef]
24. Pathak, A.K.; Singh, V.K.; Ghosh, S.; Rahman, B.M.A. Investigation of a SPR based refractive index sensor using a single mode fiber with a large D shaped microfluidic channel. *OSA Contin.* **2019**, *2*, 3008–3018. [CrossRef]
25. Patnaik, A.; Senthilnathan, K.; Jha, R. Graphene-Based Conducting Metal Oxide Coated D-Shaped Optical Fiber SPR Sensor. *IEEE Photon Technol. Lett.* **2015**, *27*, 2437–2440. [CrossRef]
26. Yundong, L.; Xili, J.; Shuguang, L.; Zhen, Z.; Ying, G.; Jie, W.; Shun, W. High sensitivity surface plasmon resonance sensor based on D-shaped photonic crystal fiber with circular layout. *Opt. Fiber Technol.* **2018**, *46*, 311–317.
27. Yasli, A.; Ademgil, H.; Haxha, S.; Aggoun, A. Multi-Chanel photonic crystal fiber based surface plasmon resonance sensor for multi-analyte sensor. *IEEE Photonics J.* **2020**, *12*, 1–15. [CrossRef]